

# Associated charm production in neutrino–nucleus interactions

The CHORUS Collaboration

A. Kayis-Topaksu<sup>1</sup>, G. Öngüt<sup>1</sup>, R. van Dantzig<sup>2</sup>, M. de Jong<sup>2</sup>, R.G.C. Oldeman<sup>2,25</sup>, M. Güler<sup>3,a</sup>, U. Köse<sup>3</sup>, P. Tolun<sup>3</sup>, M.G. Catanesi<sup>4</sup>, M.T. Muciaccia<sup>4</sup>, K. Winter<sup>5</sup>, B. Van de Vyver<sup>6,26,b</sup>, P. Vilain<sup>6,c</sup>, G. Wilquet<sup>6,c</sup>, B. Saitta<sup>7</sup>, E. Di Capua<sup>8</sup>, S. Ogawa<sup>9</sup>, H. Shibuya<sup>9</sup>, I.R. Hristova<sup>10,27</sup>, T. Kawamura<sup>10</sup>, D. Kolev<sup>10,d</sup>, H. Meinhard<sup>10</sup>, J. Panman<sup>10</sup>, A. Rozanov<sup>10,28</sup>, R. Tsenov<sup>10,d</sup>, J.W.E. Uiterwijk<sup>10</sup>, P. Zucchelli<sup>10,26,e</sup>, J. Goldberg<sup>11</sup>, M. Chikawa<sup>12</sup>, J.S. Song<sup>13</sup>, C.S. Yoon<sup>13</sup>, K. Kodama<sup>14</sup>, N. Ushida<sup>14</sup>, S. Aoki<sup>15</sup>, T. Hara<sup>15</sup>, T. Delbar<sup>16</sup>, D. Favart<sup>16</sup>, G. Grégoire<sup>16</sup>, S. Kalinin<sup>16</sup>, I. Makhlioueva<sup>16</sup>, A. Artamonov<sup>17</sup>, P. Gorbunov<sup>17,26</sup>, V. Khovansky<sup>17</sup>, V. Shamanov<sup>17</sup>, I. Tsukerman<sup>17</sup>, N. Bruski<sup>18</sup>, D. Frekers<sup>18</sup>, K. Hoshino<sup>19</sup>, J. Kawada<sup>19</sup>, M. Komatsu<sup>19</sup>, M. Miyanishi<sup>19</sup>, M. Nakamura<sup>19</sup>, T. Nakano<sup>19</sup>, K. Narita<sup>19</sup>, K. Niu<sup>19</sup>, K. Niwa<sup>19</sup>, N. Nonaka<sup>19</sup>, O. Sato<sup>19</sup>, T. Toshito<sup>19</sup>, S. Buontempo<sup>20</sup>, A.G. Cocco<sup>20</sup>, N. D'Ambrosio<sup>20</sup>, G. De Lellis<sup>20</sup>, G. De Rosa<sup>20</sup>, F. Di Capua<sup>20</sup>, G. Fiorillo<sup>20</sup>, A. Marotta<sup>20</sup>, P. Migliozi<sup>20</sup>, L. Scotto Lavina<sup>20</sup>, P. Strolin<sup>20</sup>, V. Tioukov<sup>20</sup>, T. Okusawa<sup>21</sup>, U. Dore<sup>22</sup>, P.F. Loverre<sup>22</sup>, L. Ludovici<sup>22</sup>, G. Rosa<sup>22</sup>, R. Santacesaria<sup>22</sup>, A. Satta<sup>22</sup>, F.R. Spada<sup>22</sup>, E. Barbuto<sup>23</sup>, C. Bozza<sup>23</sup>, G. Grella<sup>23</sup>, G. Romano<sup>23</sup>, C. Sirignano<sup>23</sup>, S. Sorrentino<sup>23</sup>, Y. Sato<sup>24</sup>, I. Tezuka<sup>24</sup>

<sup>1</sup> Çukurova University, Adana, Turkey

<sup>2</sup> NIKHEF, Amsterdam, The Netherlands

<sup>3</sup> Physics Department of Middle East Technical University, 06531 Ankara, Turkey

<sup>4</sup> Università di Bari and INFN, Bari, Italy

<sup>5</sup> Humboldt Universität, Berlin, Germany<sup>f</sup>

<sup>6</sup> Inter-University Institute for High Energies (ULB-VUB) Brussels, Brussels, Belgium

<sup>7</sup> Università di Cagliari and INFN, Cagliari, Italy

<sup>8</sup> Università di Ferrara and INFN, Ferrara, Italy

<sup>9</sup> Toho University, Funabashi, Japan

<sup>10</sup> CERN, Geneva, Switzerland

<sup>11</sup> Technion, Haifa, Israel

<sup>12</sup> Kinki University, Higashiosaka, Japan

<sup>13</sup> Gyeongsang National University, Jinju, Korea

<sup>14</sup> Aichi University of Education, Kariya, Japan

<sup>15</sup> Kobe University, Kobe, Japan

<sup>16</sup> Université Catholique de Louvain, Louvain-la-Neuve, Belgium

<sup>17</sup> Institute for Theoretical and Experimental Physics, Moscow, Russian Federation

<sup>18</sup> Westfälische Wilhelms-Universität, Münster, Germany<sup>f</sup>

<sup>19</sup> Nagoya University, Nagoya, Japan

<sup>20</sup> Università Federico II and INFN, Naples, Italy

<sup>21</sup> Osaka City University, Osaka, Japan

<sup>22</sup> Università La Sapienza and INFN, Rome, Italy

<sup>23</sup> Università di Salerno and INFN, Salerno, Italy

<sup>24</sup> Utsunomiya University, Utsunomiya, Japan

<sup>25</sup> Now at Università di Cagliari, Cagliari, Italy

<sup>26</sup> Now at SpinX Technologies, Geneva, Switzerland

<sup>27</sup> Now at DESY, Hamburg, Germany

<sup>28</sup> Now at CPPM CNRS-IN2P3, Marseille, France

Received: 11 May 2007 / Revised version: 21 August 2007 /

Published online: 15 September 2007 – © Springer-Verlag / Società Italiana di Fisica 2007

**Abstract.** In this paper a search for associated charm production both in neutral and charged current  $\nu$ -nucleus interactions is presented. The improvement of automatic scanning systems in the CHORUS experiment allows an efficient search to be performed in emulsion for short-lived particles. Hence a search for rare processes, like the associated charm production, becomes possible through the observation of the double charm-decay topology with a very low background. About 130 000  $\nu$  interactions located in the emulsion target have been analysed. Three events with two charm decays have been observed in the neutral-current sample with an estimated background of  $0.18 \pm 0.05$ . The relative rate of the associated charm cross-section in deep inelastic  $\nu$  interactions,  $\sigma(c\bar{c}\nu)/\sigma_{\text{NC}}^{\text{DIS}} = (3.62_{-2.42}^{+2.95}(\text{stat}) \pm 0.54(\text{syst})) \times 10^{-3}$  has been measured. One event with two charm decays has been observed in charged-current  $\nu_{\mu}$  interactions with an estimated background of  $0.18 \pm 0.06$  and the upper limit on associated charm production in charged-current interactions at 90% C.L. has been found to be  $\sigma(c\bar{c}\mu^{-})/\sigma_{\text{CC}} < 9.69 \times 10^{-4}$ .

## 1 Introduction

The production of two charmed particles in neutrino–nucleon scattering is a very rare process and therefore difficult to measure. The charm pair originates from two different processes: one, the so-called boson-gluon fusion mechanism, is possible only in neutral-current interactions, while the other, gluon bremsstrahlung, occurs both in neutral and charged current (NC and CC) interactions. The Feynman diagrams of both process are shown in Fig. 1.

In early neutrino experiments at the CERN SPS and Fermilab, measurements of production rates of prompt trimuons [1–3] and like-sign dimuons [4–7] were found to be higher than expected [8]. In the past the origin of these events was assumed to be the associated charm production in CC neutrino interactions with subsequent muonic decay of the charmed particle(s):

$$\nu_{\mu}N \rightarrow \mu^{-}c\bar{c}X, \quad (1)$$

where the charm–anticharm pair is produced by a gluon emitted via bremsstrahlung from a light parton. More recently, an analysis by CHORUS [9] suggested a significant contribution from  $\mu^{+}\mu^{-}$  decays of light vector mesons. In a previous search, based on the visual observation of the charmed hadron decays, the CHORUS collaboration has published the first evidence for this process [10] through the observation of one event.

For the NC process, the E531 experiment reported the observation of one event with two neutral decay topology. Using this event and correcting for the efficiency, a relative rate was quoted as  $\frac{\sigma(\nu_{\mu} \rightarrow c\bar{c}\nu_{\mu})}{\sigma(\nu_{\mu} \rightarrow \nu_{\mu})} = (1.3_{-1.1}^{+3.1}) \times 10^{-3}$  [11] at the average neutrino beam energy of 22 GeV. No background estimation was given.

A measurement of this rate was recently made by the NuTeV experiment [12, 13] through the detection of events with wrong sign muon final states. The analysis technique consists in comparing the visible inelasticity,  $y_{\text{vis}} =$

$E_{\text{HAD}}/(E_{\text{HAD}} + E_{\mu})$ , measured in the  $\nu_{\mu}$  and  $\bar{\nu}_{\mu}$  data samples where the leading muon had the wrong sign of charge, to a Monte Carlo simulation containing all known conventional wrong sign muon sources and a possible NC charm signal. The NC charm signal peaks at large values of  $y_{\text{vis}}$  because the muon from the decay of a heavy flavor hadron is usually much less energetic than the hadron shower produced in the NC interaction. After consideration of all background sources, a production cross section  $\frac{\sigma(\nu_{\mu} \rightarrow c\bar{c}\nu_{\mu})}{\sigma(\nu_{\mu} \rightarrow \nu_{\mu})} = (6.4_{-4.6}^{+5.5}) \times 10^{-3}$  [12, 13] at the average neutrino beam energy of 154 GeV was obtained. More details both on the theoretical and experimental aspects of associated charm production may be found in [14, 15] and references in them.

All the results, available to date, with the exception those from E531, were extracted from multi-muon samples with a large background of non prompt muons. In the CHORUS experiment a different search for associated charm production in NC and CC  $\nu_{\mu}$  interactions was carried out in nuclear emulsion, is practically background free and is presented in this paper. The search is based on the visual observation of the primary vertex and the two decay vertices, taking advantage of the sub-micrometric position resolution of the nuclear emulsion. We report the observation of four events with two charm decays: three in NC and one in CC  $\nu_{\mu}$  interactions. Based on the observed events, taking care of the estimated background and correcting for the detection efficiencies, we obtain a production rate of associated charm in NC interactions and an upper limit for the CC process.

## 2 The experimental apparatus

The CHORUS detector is a hybrid setup that combines a nuclear emulsion target with various electronic detectors, as described in [16].

A three-dimensional reconstruction of the decays of short-lived particles such as the  $\tau$  lepton and charmed hadrons can be performed in nuclear emulsions. The emulsion target is segmented into four stacks with an overall mass of 770 kg. Each of the stacks consists of eight modules of 36 plates of 36 cm  $\times$  72 cm size. Each plate consists of a 90  $\mu\text{m}$  plastic support coated on both sides with a 350  $\mu\text{m}$  emulsion layer [17]. Each stack is followed by three emulsion sheets, having a 90  $\mu\text{m}$  emulsion layer on both sides of an 800  $\mu\text{m}$  thick plastic base, acting as an interface to

<sup>a</sup> e-mail: mguler@mail.cern.ch

<sup>b</sup> Fonds voor Wetenschappelijk Onderzoek, Belgium

<sup>c</sup> Fonds National de la Recherche Scientifique, Belgium

<sup>d</sup> On leave of absence and at St. Kliment Ohridski University of Sofia, Bulgaria

<sup>e</sup> On leave of absence from INFN, Ferrara, Italy

<sup>f</sup> Supported by the German Bundesministerium für Bildung und Forschung under contract numbers 05 6BU11P and 05 7MS12P.

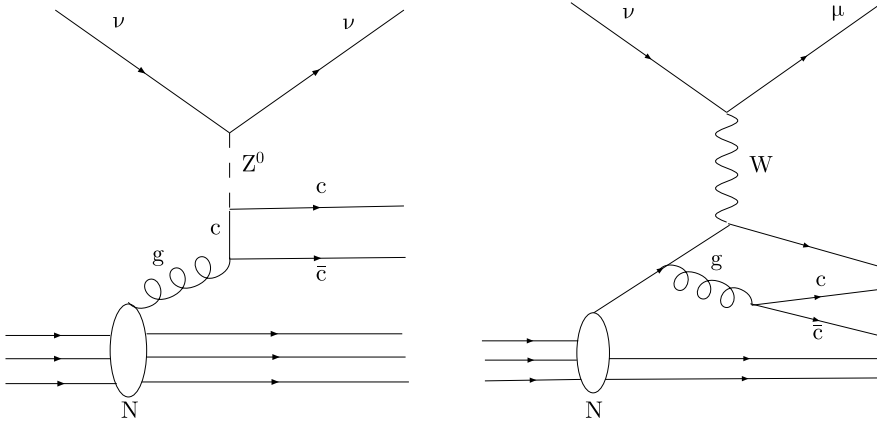


**Fig. 1.** Feynman diagrams for boson-gluon fusion (*left*) and gluon bremsstrahlung processes (*right*)

a set of scintillating fibre tracker planes. The accuracy of the fibre tracker predictions is about  $150\ \mu\text{m}$  in track position and  $2\ \text{mrad}$  in angle. The interface sheets and the fibre trackers provide accurate particle trajectory predictions in the emulsion stack in order to locate the interaction vertex. The information of the electronic detectors has been used to define two data sets, the  $1\mu$  and  $0\mu$  samples. The events belonging to the  $1\mu$  sample contain one reconstructed muon of negative charge. The muon identification and reconstruction is based on the muon spectrometer response. The  $0\mu$  sample contains events where no muon is found. It mainly consists of NC  $\nu_\mu$  interactions with a contamination of mis-identified CC  $\nu_\mu$  interactions and interactions generated by neutrinos other than  $\nu_\mu$ .

The emulsion scanning is performed by fully automated microscopes equipped with CCD cameras and a read out system called “Ultra Track Selector” [18]. In order to recognize the track segments in the emulsion, a series of tomographic images are taken by moving the focus at different depths in the emulsion thickness. The digitized images are shifted according to the predicted track angle and then added. The presence of aligned grains forming a track is detected as a local peak above the gray level of the summed image. The track finding efficiency of the track selector is higher than 98% for track angles up to  $400\ \text{mrad}$  with respect to normal incidence.

The electronic detectors downstream of the emulsion target include a hadron spectrometer which measures the bending of charged particles in an air-core magnet, a calorimeter where the energy and direction of showers are measured and a muon spectrometer which measures the charge and momentum of muons. In this analysis, the momentum of particles other than muons in the candidate events were determined by measuring their multiple scattering in the emulsion target.

### 3 Event samples and selection of two charm topologies

The west area neutrino facility (WANF) at CERN provided a wide band beam of  $27\ \text{GeV}$  average energy consisting mainly of  $\nu_\mu$ , with a contamination of  $5.1\%$   $\bar{\nu}_\mu$ ,

$0.8\%$   $\nu_e$  and  $0.2\%$   $\bar{\nu}_e$ . During the four years of CHORUS operation the emulsion target has been exposed to the beam for an integrated intensity which corresponds to  $5.06 \times 10^{19}$  protons on target. The data from the electronic detectors have been analyzed and the set of events possibly originating in the emulsion stacks has been identified.

**Table 1.** Results of the visual inspection in the selected  $0\mu$  sample

Charm candidates		Rejected events	
Topology	Events	Category	Events
V2	145	Low momentum	72
V4	43	Traversing tracks	108
C1	80	$h^\pm$ int.	110
C3	75	$h^0$ int.	4
C5	4	$\gamma$ - conversion	36
V2+V2	1	Overlay secondary vertices	37
C1+V2	1		
C3+V4	1		
Total	350		367

**Table 2.** Results of the visual inspection in the selected  $1\mu$  sample

Charm candidates		Rejected events	
Topology	Events	Category	Events
V2	841	Low momentum	140
V4	230	Traversing tracks	149
V6	3	$h^\pm$ int.	258
C1	462	$h^0$ int.	69
C3	501	$\gamma$ - conversion	101
C5	23	Overlay secondary vertices	36
C1+C3	1		
C1+V2	1		
V2+V4	1		
Total	2063		753

In total about 130 000  $\nu$  events have been located in emulsion with a procedure described in [19]. In order to identify a charm decay, a volume of  $1.5 \text{ mm} \times 1.5 \text{ mm} \times 6.3 \text{ mm}$  around the located vertex position is scanned. The parameters of all track segments with angles below 400 mrad found in this volume are stored in a database. Typically, five thousand track segments are recorded per event. This procedure is called “Netscan” [20]. A detailed description of the procedure and of the algorithms used to reconstruct the event topology are given in [21, 22].

Track segments collected in the Netscan fiducial volume are analysed off-line to reconstruct the complete event topology: segments from different plates are combined into tracks; low-energy tracks are filtered out as well as track originating from outside the volume (mainly passing-through beam muons).

Possible vertices are then defined, requiring that the minimum distance between tracks attached to a common vertex is compatible with zero within errors. If several vertices are reconstructed, the primary vertex is defined, for the  $1\mu$  sample, as the one to which the muon track is attached. For the  $0\mu$  sample, the primary vertex is chosen as the most upstream one with at least one track matching one of the tracks reconstructed in the electronic detectors. Events for which the emulsion tracks do not converge to a single common vertex potentially contain a short-lived particle decay topology. They were selected for further inspection if one of the following selection criteria is satisfied [21, 22]:

- Two or more multi-tracks vertices are reconstructed.
- At least one track of the primary vertex is not reconstructed up to the edge of the Netscan volume

**Table 3.** General features of the associated charm candidates. Ns(Ns<sup>\*</sup>) and Nh stand for number of shower (reconstructed in the electronic detector) and heavily ionizing tracks at the neutrino interaction vertex.  $E_{\text{sh}}$  is the hadronic shower energy,  $p_{\mu}$  the muon momentum and  $\theta_{\mu}(y,z)$  the angle between the muon and the beam directions, respectively in the horizontal and vertical planes. No correction was made for the energy of the two neutrinos from the charm decays

	Event Id	Ns (Ns <sup>*</sup> )	Nh	$E_{\text{sh}}$ (GeV)	$p_{\mu}$ (GeV/c)	$\theta_{\mu}(y,z)$ (rad)
NC	8132-12312	1(1)	2	38.2		
	7692-5575	2(1)	0	47.1		
	7739-3952	6(1)	1	45.9		
CC	7904-4944	4(2)	0	42.5	17.6	(−0.164, 0.080)

**Table 4.** General features of the charged daughter particles in the associated charm candidates.  $M_{\text{min}}$  stands for minimum mass at 90% C.L. of the parent particle.  $\theta(y,z)$  is the angle between the charged daughter particle and the beam directions, respectively in the horizontal and vertical planes,  $p$  is the momentum of the charged daughter particle measured using multiple Coulomb scattering. (The momentum measurement was not applied to event 7739-3952 and failed for two daughters of V4 decay in event 7739-3952.)

	Event Id	Topology	$M_{\text{min}}$ (GeV)	$\theta(y,z)$ (rad)	$p$ (GeV/c)	
NC	8132-12312	V2	0.80	(0.049, −0.026)	4.66	
				(−0.023, 0.040)	1.39	
	7692-5575	V2	0.95	(−0.165, 0.045)	2.72	
				(0.034, 0.105)	3.33	
				(0.026, −0.056)	4.11	
				(0.082, 0.032)	3.81	
7739-3952	C1			(−0.136, 0.291)	1.82	
				(0.129, −0.072)		
	V4				(−0.005, −0.064)	
					(0.083, 0.042)	
					(0.075, 0.336)	
					(0.011, −0.038)	
C3				(−0.071, 0.238)		
				(−0.294, −0.376)		
CC	7904-4944	V4		(0.007, −0.087)	1.92	
				(−0.045, −0.001)	2.32	
				(0.269, 0.305)		
	V2	0.81			(0.101, −0.169)	
					(0.029, −0.053)	4.70
					(0.001, 0.289)	0.67

- A track originating in the same plate as the primary vertex has an impact parameter IP relative to it satisfying the two conditions:

- $IP > \sqrt{(5.0^2 + (2dx \times \sigma)^2)} \mu\text{m}$  where  $\sigma = \sqrt{(0.003^2 + (0.0194 \times \tan\theta)^2)}$  is a parameterization of the angular error and  $dx$  is the distance of the vertex from the most upstream daughter track segment.
- $IP < 750 \mu\text{m}$ , to reject spurious tracks not related to the neutrino interaction.

After selection, the samples of 26 621  $0\mu$  and 99 245  $1\mu$  events reduce to respectively 717 and 2816 events. These are then visually inspected to confirm the decay topology. A secondary vertex is accepted as decay if the number of prongs is consistent with charge conservation and no evidence for hadronic interaction, e.g. Auger electron, nuclear recoil or break up, is observed. Decays into a single charged particle (so called kink) are accepted only if the angle between the parent and daughter tracks is greater than 50 mrad and the length of the parent track is greater than 25  $\mu\text{m}$ .

The observable decay topologies are classified according to their numbers of charged decay products into C1, C3 or C5 for the charged and V2, V4 or V6 for neutral decay particles. The result of the visual inspection is given in Tables 1 and 2 for the  $0\mu$  and the  $1\mu$  samples respectively. In both the  $0\mu$  and the  $1\mu$  samples, three events have been observed with two charm-decay topology.

The rejected sample consists mainly of low momentum tracks for which the multiple scattering leads to a fake impact parameter or to a failure to reconstruct the track as traversing the plate. The remaining events in the sample consist of hadronic interactions, gamma conversions

and overlay secondary vertices, reconstructed using one or more background tracks or of vertices with a parent track not connected to the primary vertex.

After topological confirmation of the decays, further kinematical selections are applied in order to eliminate the background coming from strange particle decays and from hadronic interactions. In case of a C1 topology, the requirement  $p_T > 0.25 \text{ GeV}/c$  on the transverse momentum of the daughter particle with respect to the parent direction is applied. This cut also reduces significantly the background caused by “white kinks”, i.e. single prong hadronic interaction without emission of any heavily ionizing particle, Auger electron or other evidence for nuclear recoil or break up. The selection criterion applied to V2 decays is  $\phi > 10 \text{ mrad}$ , where the angle  $\phi$  measures the acoplanarity between the parent direction and the plane formed by the charged decay products. This cut eliminates mainly the two-body decays of neutral strange particles. The effects of these kinematical cuts are included in the determination of the Netscan efficiencies.

Four events satisfied the above selection criteria. Their general features are listed in Tables 3 and 4.

## 4 The candidate events in the NC sample

In the NC sample three candidates for associated charm production satisfied the above selection criteria. A description of each event is given below.

Event 8132-12312 with a V2+V2 decay topology is sketched in Fig. 2 and microscope view of the event in the emulsion at relevant positions is shown in Fig. 3. Only one minimum-ionizing (shower) particle is emitted from the primary vertex and is identified as a hadron in the elec-

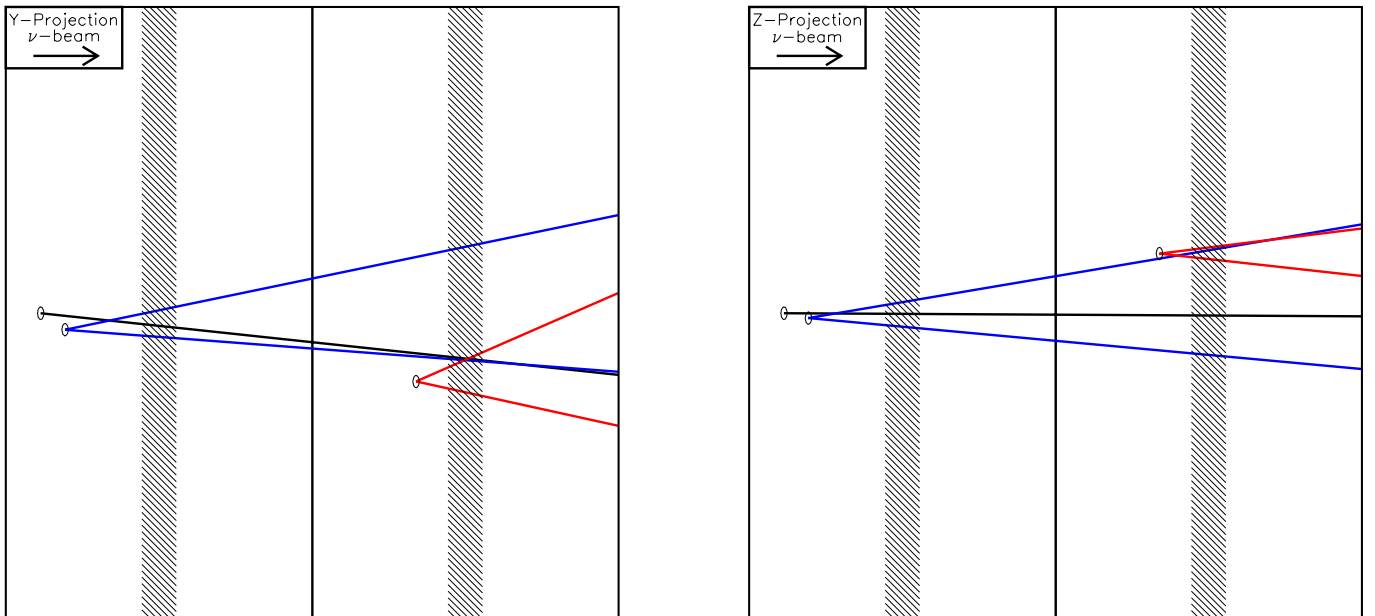


**Fig. 2.** Sketch of the NC event, (8132-12312) with a V2+V2 topology (the shaded area is the 90  $\mu\text{m}$  plastic base between the two 350  $\mu\text{m}$  emulsion layers)

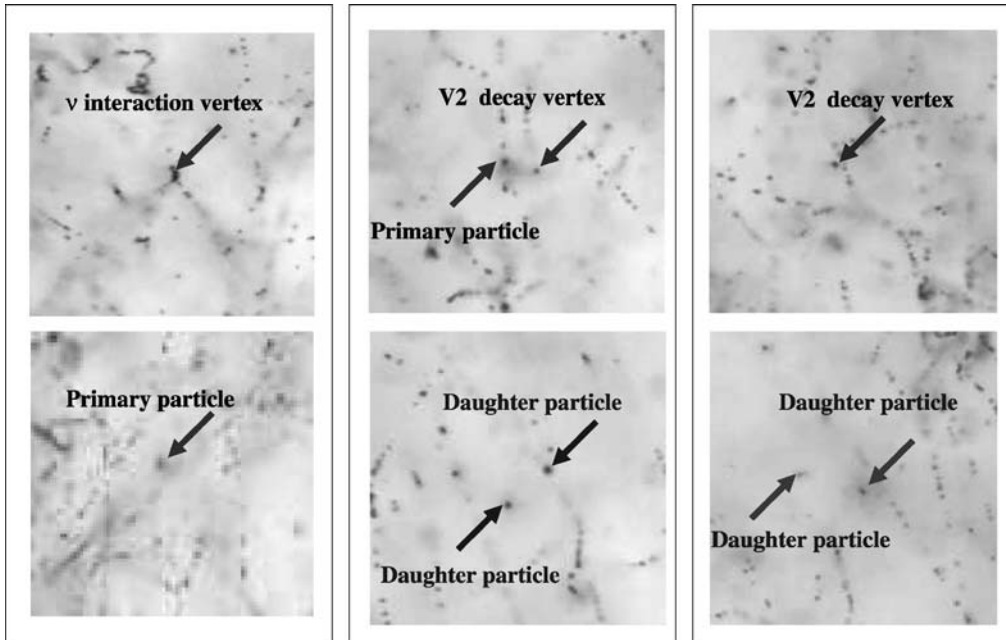


**Fig. 3.** Microscope views of event 8132-12312 taken in the emulsion. Since the neutrino beam is perpendicular to the emulsion target, the trajectory of a charged particle appears as a ‘dot’. The *top-left picture* shows the neutrino interaction vertex. A charged particle which is visible several microns downstream of the vertex emerges from the neutrino vertex. The *top-center picture* shows the decay vertex of a neutral charmed particle decaying into two charged particles (V2) 63  $\mu\text{m}$  downstream of the primary vertex. The trajectory of the daughter particles is visible at *bottom-center picture*. A second V2 decay topology is found 977  $\mu\text{m}$  downstream of the primary vertex as shown in the *top-right picture*. In the *bottom-right picture* the trajectory of daughter particles from the second neutral decay becomes visible after several microns downstream of the decay vertex

tronic detector. In the same emulsion plate, a neutral particle decays into two charged particles (V2) 63  $\mu\text{m}$  downstream of the primary vertex. Both daughter tracks are reconstructed in the electronic detector. The acoplanarity of parent and daughter tracks,  $\phi = 24.2 \text{ mrad} \pm 5.3 \text{ mrad}$  rules out a two body decay. Moreover, the lower limit of the mass  $M_{\text{min}}$  of the parent particle is measured to be 0.80 GeV (at 90% C.L.). In one plate downstream, a second V2 decay has been located, 977  $\mu\text{m}$  from the primary vertex. The acoplanarity angle  $\phi$  and the minimum mass  $M_{\text{min}}$  are measured to be  $36.1 \text{ mrad} \pm 0.3 \text{ mrad}$  and 0.95 GeV (at 90% C.L.) respectively.

Event 7692-5575 (with a C1+V2 decay topology): At the primary vertex there are two shower tracks, one of which decaying after 163  $\mu\text{m}$  into a charged particle (C1) with a 0.179 rad kink angle. The daughter momentum was measured by multiple scattering to be larger than 1.82 GeV/ $c$  (at 90% C.L.). Its transverse momentum  $p_T$  with respect to its parent is larger than 0.32 GeV/ $c$  (at 90% C.L.), which rules out the hypothesis of a strange particle decay. In the same emulsion plate, 224  $\mu\text{m}$  from the primary vertex, a second decay with a V2 topology has been observed; the decay vertex occurs however in the plastic base. The acoplanarity angle is  $14.9 \text{ mrad} \pm 1.5 \text{ mrad}$  and  $M_{\text{min}} = 0.68 \text{ GeV}$  (at 90% C.L.) These values are inconsistent with a strange-particle decay hypothesis.

Event 7739-3952 (with a C3+V4 decay topology): The primary vertex has six shower tracks, none of them identified as a muon. One of the shower tracks decays after

426  $\mu\text{m}$  into three charged particles while the V4 decay vertex is 884  $\mu\text{m}$  from the primary vertex.

## 5 The candidate event in the CC sample

Out of the three double charm candidates of Table 2, two are rejected on the basis of the  $p_T$  cut at their C1 vertex. The remaining event 7904-4944 is shown in Fig. 4. The primary vertex is located 200  $\mu\text{m}$  from the plate downstream surface. There are four primary shower tracks; one of them is identified as a negative muon in the spectrometer. In the same plate, 58  $\mu\text{m}$  downstream of the primary vertex, a neutral particle decays into a V2 topology. Both daughter tracks are reconstructed in the electronic detector. The acoplanarity angle  $\phi$  is  $12.8 \text{ mrad} \pm 1.5 \text{ mrad}$ , and the minimum mass of the parent particle,  $M_{\text{min}} = 0.81 \text{ GeV}$  at 90% C.L. A second neutral particle decays into a V4 topology with a flight length of 761  $\mu\text{m}$  from the primary vertex. Two of four daughter tracks are reconstructed in the electronic detector.

In [10], we have reported the observation of one event in CC  $\nu_\mu$  interactions based on a subset of the data (about 50% of the present sample). This search was based on different selection criteria and was performed before the development of the Netscan technique: charged particles at the primary vertex were followed down manually to find decay vertices. This event has not been retrieved in the

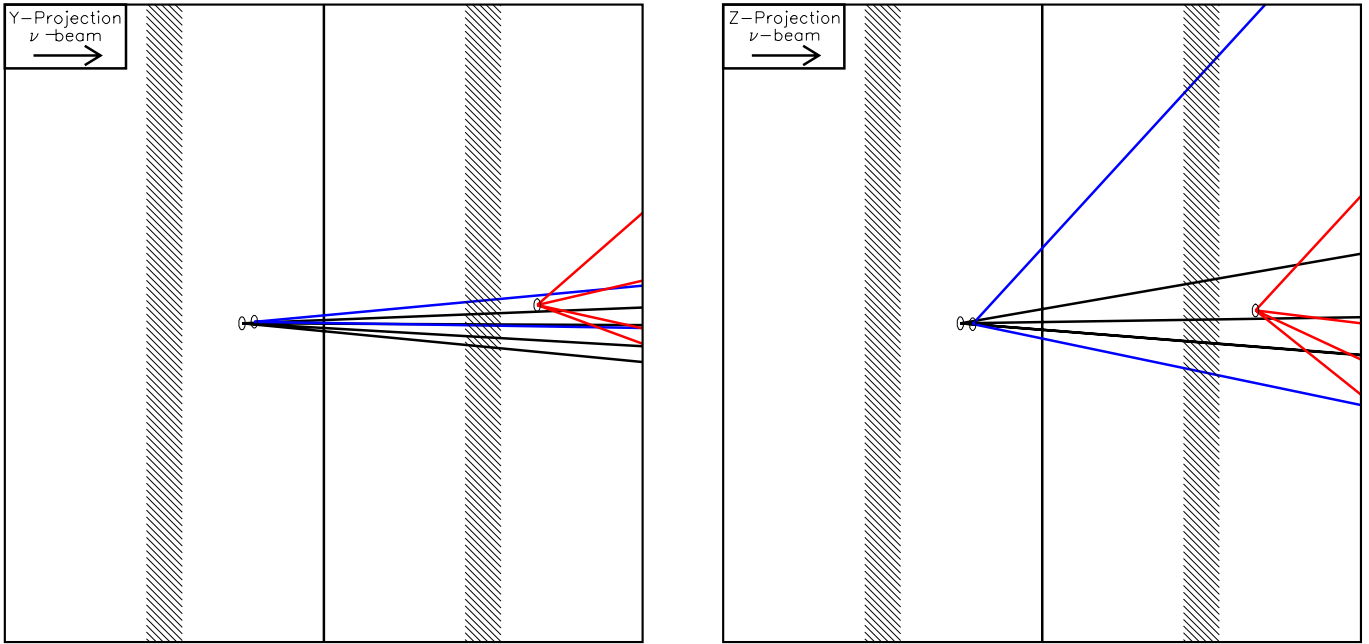


**Fig. 4.** Sketch of CC event (7904-4944) with a V2+V4 topology (the shaded area is the 90  $\mu\text{m}$  plastic base between the two 350  $\mu\text{m}$  emulsion layers)

present analysis because the emission angle of the charm daughter is out of the angular acceptance of the Netscan procedure.

## 6 Evaluation of the reconstruction efficiency

Large samples of neutrino interactions were generated with a neutrino energy distribution according to the beam spectrum using the HERWIG event generator [23], with the leading-order parton distribution functions of MRST [24]. This generator produces associated charm-production events in both neutral-current and charged-current interactions. Efficiencies and backgrounds were evaluated with a simulation of the detector based on GEANT3 [25].

The simulated response of the electronic detectors is processed through the same reconstruction program as the one used for the data. The tracks in emulsion and the performance of the UTS are also simulated, in order to evaluate the efficiency of the scanning procedure.

In order to evaluate the Netscan procedure efficiency, one needs to reproduce realistic track densities. This was achieved by merging the emulsion data of the simulated events with real Netscan data which do not have a reconstructed vertex but contain tracks which stop or pass through the Netscan fiducial volume, representing the real experimental background [26]. The combined data are passed through the same Netscan reconstruction and selection programs as used for the real data. The average detection efficiencies for NC and CC sample are evaluated to be  $(12.8 \pm 0.6)\%$  and  $(8.5 \pm 0.6)\%$ , respectively.

The ratio of the reconstruction and location efficiency of the NC  $c\bar{c}$  events to that of the whole sample of NC

events is found to be  $0.496 \pm 0.022$ . This ratio is  $0.506 \pm 0.018$  in the CC channel.

The lower reconstruction and location efficiency of  $c\bar{c}$  events is due to the larger hadronic activity in the electronic detector for these events.

## 7 Background evaluation

The search is essentially topological even if there are additional measurements of the momentum and acoplanarity angle to further validate the candidates. In Table 5 we list all relevant background sources for double charm production in CC interactions.

A double charm event is topologically indistinguishable from a single charm event with a primary non-charmed hadron which undergoes either a decay or an interaction without any visible recoil of the nuclei. Among the strange hadrons produced in a single charm event, the  $\Sigma^\pm$  has the lowest  $c\tau$  (a few cm) and is relatively abundant (about 1%). Owing to longer decay lengths there are negligible contributions from decays of other non-charmed hadrons like kaons and pions.

Decays of strange neutral particles like  $\Lambda$  and  $K_s^0$  do not give a sizeable contribution owing to the acoplanarity cut.

The interaction length for white interactions is very large, ranging from a few metres for single prong interactions to several hundred metres for multi-prong interactions. A simulation of these processes using FLUKA [27] has been carried out and the interaction lengths for the different processes have been obtained. In the course of the CHORUS analysis, 243 m of charged hadron tracks have been followed and 26 white interactions [19] have

**Table 5.** Background sources and the corresponding event yields in the  $1\mu$  sample

Primary interaction	secondary vertex	event yield
$\nu_\mu N \rightarrow \mu^- c \Sigma^\pm X$	$\Sigma^\pm \rightarrow 1$ prong	$0.002 \pm 0.001$
$\nu_\mu N \rightarrow \mu^- c h^\pm X$	$h^\pm$ white C1	$0.08 \pm 0.04$
$\nu_\mu N \rightarrow \mu^- c h^\pm X$	$h^\pm$ white C3	$0.06 \pm 0.04$
$\nu_\mu N \rightarrow \mu^- c h^\pm X$	$h^\pm$ white C5	$0.024 \pm 0.009$
$\nu_\mu N \rightarrow \mu^- c h^0 X$	$h^0$ white V2	$0.01 \pm 0.01$
$\nu_\mu N \rightarrow \mu^- c h^0 X$	$h^0$ white V4	$0.006 \pm 0.006$
Total		$0.18 \pm 0.06$

**Table 6.** Background sources and the corresponding event yields in the  $0\mu$  sample where  $\mu^\pm(e^\pm)$  is misidentified

Primary interaction	secondary vertex	event yield
$\nu N \rightarrow \mu^\pm(e^\pm) c \Sigma^\pm X$	$\Sigma^\pm \rightarrow 1$ prong	$0.0003 \pm 0.0001$
$\nu N \rightarrow \mu^\pm(e^\pm) c h^\pm X$	$h^\pm$ white C1	$0.013 \pm 0.005$
$\nu N \rightarrow \mu^\pm(e^\pm) c h^\pm X$	$h^\pm$ white C3	$0.011 \pm 0.005$
$\nu N \rightarrow \mu^\pm(e^\pm) c h^\pm X$	$h^\pm$ white C5	$0.004 \pm 0.001$
$\nu N \rightarrow \mu^\pm(e^\pm) c h^0 X$	$h^0$ white V2	$0.001 \pm 0.001$
$\nu N \rightarrow \mu^\pm(e^\pm) c h^0 X$	$h^0$ white V4	$0.0006 \pm 0.0006$
$\nu N \rightarrow \mu^\pm(e^\pm) c \bar{c} X$	$c\bar{c} \rightarrow$ any prong	$0.146 \pm 0.051$
Total		$0.18 \pm 0.05$

been collected, which allows a cross-check of the simulation at the 35% level. An overall background of  $0.18 \pm 0.06$  events is expected in CC interactions, mainly from white interactions.

In Table 6 are listed the background sources and the corresponding event yield in the  $0\mu$  sample. An overall background of  $0.18 \pm 0.05$  events is estimated. The main background source for the double charm production in NC interaction comes from charged lepton misidentification in CC double charm events. This background is estimated by scaling the candidate event in CC interactions with the CC contamination in  $0\mu$  sample which is estimated to be about 14%.

## 8 Results and conclusions

In summary, in a sample of 99 245  $1\mu$  events, one event has decay topologies that meet the requirements for associated charm production. The total background in the CC sample is estimated to be  $0.18 \pm 0.06$  events. In the sample of 26 621  $0\mu$  events, three events showed decay topologies that are consistent with associated charm production. The total background in the NC sample is estimated to be  $0.18 \pm 0.05$ .

In order to estimate the associated charm production rate in  $\nu_\mu$  interactions, an additional weight factor needs to be applied to  $1\mu$  events with  $p_\mu > 30$  GeV/ $c$ , since a small fraction of this category was not located and analysed. This factor was evaluated from the measured ratio  $0.305 \pm$

$0.002$  of  $1\mu$  events with  $p_\mu > 30$  GeV/ $c$  to those with  $p_\mu < 30$  GeV/ $c$ ; it was found to be 1.021. In order to evaluate the real number of  $\nu$  NC we have used the measured fraction of  $0.274 \pm 0.005$  between deep-inelastic NC and CC  $\nu_\mu$  interactions. This value is smaller than what was measured by CHARM, CDHS and CCFR collaborations [28–30] since a correction for the non-isoscalarity of the emulsion target is applied. In NC interactions identification of the neutrino flavor is not possible in the experiment. Therefore, the NC sample contains a small fraction of  $\nu_e$ ,  $\bar{\nu}_e$  and  $\bar{\nu}_\mu$  NC interactions. The contribution of neutrino flavors other than  $\nu_\mu$  to the normalization is estimated to be 3.3%. Since in CC interactions at least one reconstructed muon in the spectrometer is required both NC and CC interactions have a similar energy threshold which is about 6 GeV.

The relative rate of NC associated charm production is given by

$$\frac{\sigma(c\bar{c}\nu)}{\sigma_{\text{NC}}^{\text{DIS}}} = \left( \frac{N_{\text{obs}}^{c\bar{c}} - N_{\text{bgr}}}{R_{\text{NC}}^{\text{CC}} N_{\text{CC}}} \right) \frac{1}{r_{\text{loc}}} \frac{1}{\epsilon_{\text{net}}}.$$

Where:

- $N_{\text{obs}}^{c\bar{c}} = 3$  is the number of candidate events in the  $0\mu$  sample;
- $N_{\text{bgr}} = 0.18 \pm 0.05$  is the total background in NC sample;
- $R_{\text{NC}}^{\text{CC}} = 0.285 \pm 0.005$  is the effective ratio between deep-inelastic NC and CC interactions;
- $N_{\text{CC}} = 101\,329$  is the number of CC  $\nu_\mu$  interactions;
- $\epsilon_{\text{net}} = 0.128 \pm 0.006$  is the average detection efficiency for the NC  $c\bar{c}$  sample;
- $r_{\text{loc}} = 0.211 \pm 0.004$  is the ratio of the reconstruction and location efficiency of events with  $c\bar{c}$  in NC events to that of all CC events.

The value obtained for this ratio normalizing to the total neutrino flux with 27 GeV average neutrino energy is

$$\frac{\sigma(c\bar{c}\nu)}{\sigma_{\text{NC}}^{\text{DIS}}} = (3.62_{-2.42}^{+2.95}(\text{stat}) \pm 0.54(\text{syst})) \times 10^{-3}.$$

The statistical error is derived using a 68% confidence interval in the unified approach for the analysis of small signals in the presence of background [34]. We have accounted for a systematic uncertainty of 15% coming from the efficiency estimation by Monte Carlo modeling. The energy threshold of associated charm production is significantly higher than for NC interactions. Based on the HERWIG event generator, an energy threshold cut of 35 GeV is applied to NC interactions. The relative rate of NC associated charm production is also evaluated with the energy threshold cut and found to be  $(7.30_{-4.88}^{+5.95}(\text{stat}) \pm 1.09(\text{syst})) \times 10^{-3}$ . The average neutrino energy above this threshold is 73 GeV, to be compared with the average visible energy of our candidates of 44 GeV. The neutrino spectrum for NC interactions is peaked at about 25 GeV and decreases very rapidly. Therefore, we expect events to occur close the threshold. The result is consistent with the E531 [11] and NuTeV [12, 13] measurements. The measured cross-section is consistent with our measurement on NC production of



$J/\Psi$  [31]<sup>1</sup>. Given the fact that the cross-section is predicted to have a strong energy dependence and taking into account that the neutrino energy spectrum of the beam used in this experiment peaks at values where this cross-section is predicted to be low, our result is compatible with the prediction of the  $Z^0$ -gluon fusion model [32, 33]. In the framework of this model, one obtains the relative rate of NC associated charm production as  $\sim 4 \times 10^{-3}$ .

With the observation of one event for associated charm production in CC interactions, we obtain for the relative rate an upper limit at 90% C.L. [34] of

$$\frac{\sigma(c\bar{c}\mu^-)}{\sigma_{CC}} < 9.69 \times 10^{-4},$$

normalizing to the total neutrino flux. Due to different energy thresholds in single and associated charm production, the production cross-section relative to CC interactions is estimated with the energy cut of 35 GeV. An upper limit for the relative rate with the energy threshold cut is found to be  $2.24 \times 10^{-3}$ . The average neutrino energy above this threshold is 73 GeV. Since the topology of the single candidate event is not one of the most likely background channels, it is justified to give a cross-section for this process. Based on the single event, the production cross-section relative to CC interactions is  $1.95_{-1.44}^{+3.22}(\text{stat}) \pm 0.29(\text{syst}) \times 10^{-4}$  with a systematic error of 15% from the flux normalization. The rate of CC associated charm production with the threshold cut is obtained to be  $(4.50_{-3.33}^{+7.44}(\text{stat}) \pm 0.68(\text{syst})) \times 10^{-4}$ . The cross-section predicted by the QCD inspired parton model [8] has a strong energy dependence. Although the cross-section of this process at the average energy of the CHORUS  $\nu_\mu$  beam is low, the measured production rate is in agreement with the prediction of the QCD inspired parton model. The relative rate of CC associated charm production is calculated to be  $\sim 2 \times 10^{-4}$  within the framework of this model. The a posteriori probability that the background for the topology with two neutral decays gives one event is 0.016. Taking into account that this was not the only topology searched for, it is difficult to convert this into a uniquely defined confidence level. However, given the special topology, it is very likely that this event constitutes an observation of associated charm production in CC interactions.

*Acknowledgements.* We gratefully acknowledge the help and support of our numerous technical collaborators who contributed to the detector construction and operation. We thank the neutrino beam staff for the competent assistance ensuring the excellent performance of the facility. The accumulation of a large data sample in this experiment has also been made possible thanks to the efforts of the crew operating the CERN PS and SPS. The general technical support from EP (ECP) and IT Divisions is gratefully acknowledged.

The experiment has been made possible by grants from our funding agencies: the Institut Interuniversitaire des Sciences

Nucléaires and the Interuniversitair Instituut voor Kernwetenschappen (Belgium), The Israel Science Foundation (Grant 328/94) and the Technion Vice President Fund for the Promotion of Research (Israel), CERN (Geneva, Switzerland), the German Bundesministerium für Bildung und Forschung (Grant 057MS12P(0)) (Germany), the Institute of Theoretical and Experimental Physics (Moscow, Russia), the Instituto Nazionale di Fisica Nucleare (Italy), the Promotion and Mutual Aid Corporation for Private Schools of Japan and Japan Society for the Promotion of Science (Japan), the Korea Research Foundation Grant (KRF-99-005-D00004) (Republic of Korea), the Foundation for Fundamental Research on Matter FOM and the National Scientific Research Organization NWO (The Netherlands) and the Scientific and Technical Research Council of Turkey (Turkey).

## References

1. A. Benvenuti et al., Phys. Rev. Lett. **38**, 1110 (1977)
2. B.C. Barish et al., Phys. Rev. Lett. **38**, 577 (1977)
3. T. Hansl et al., Nucl. Phys. B **142**, 381 (1978)
4. A. Benvenuti et al., Phys. Rev. Lett. **35**, 1199 (1975)
5. M. Holder et al., Phys. Lett. B **70**, 396 (1977)
6. P.H. Sandler et al., Z. Phys. C **57**, 1 (1993)
7. D. Haidt, H. Pietschmann, The handbook Landolt-Boernstein Vol. I/10, in Electroweak Interactions. Experimental Facts and Theoretical Foundation, Springer press (1988)
8. K. Hagiwara, Nucl. Phys. B **173**, 487 (1980)
9. CHORUS Collaboration, A. Kayis-Topaksu et al., Phys. Lett. B **596**, 44 (2004)
10. CHORUS Collaboration, A. Kayis-Topaksu et al., Phys. Lett. B **539**, 188 (2002)
11. E531 Collaboration, N. Ushida et al., Phys. Lett. B **206**, 375 (1988)
12. NuTeV Collaboration, M. Goncharov et al., Phys. Rev. D **64**, 112006 (2001)
13. NuTeV Collaboration, A. Alton et al., Int. J. Mod. Phys. A **16S1B**, 764 (2001)
14. G. De Lellis, PhD Thesis (Università Federico II, Napoli, 2000) (<http://choruswww.cern.ch/Reference/Theses/Theses.html>)
15. G.D. Lellis, P. Migliozi, P. Santorelli, Phys. Rep. **399**, 227 (2004) [Erratum-ibid. **411**, 323 (2005)]
16. CHORUS Collaboration, E. Eskut et. al., Nucl. Instrum. Methods A **401**, 7 (1997)
17. CHORUS Collaboration, S. Aoki et al., Nucl. Instrum. Methods A **447**, 361 (2000)
18. T. Nakano, PhD thesis (Nagoya University, Japan, 1997)
19. CHORUS Collaboration, E. Eskut et. al., Phys. Lett. B **497**, 8 (2001)
20. DONUT Collaboration, K. Kodama et al., Nucl. Instrum. Methods A **493**, 45 (2002)
21. M. Güler, PhD Thesis (METU, Ankara, 2000) (CERN-THESIS-2002-027)
22. CHORUS Collaboration, A. Kayis-Topaksu et al., Phys. Lett. B **527**, 173 (2002)
23. HERWIG 6.5, G. Corcella et al., JHEP **0101**, 010 (2001) [[hep-ph/0011363](http://arxiv.org/abs/hep-ph/0011363)], [[hep-ph/0210213](http://arxiv.org/abs/hep-ph/0210213)]
24. A.D. Martin, R.G. Roberts, W.J. Stirling, R.S. Thorne, Eur. Phys. J. C **4**, 463 (1998)
25. GEANT 3.21, CERN program library long write up W5013

<sup>1</sup> We assume that  $J/\Psi$  production is 1/6 of the total  $c\bar{c}$  production.

26. M. Güler, O. Sato, CHORUS internal Note 2000017 (2002) <http://choruswww.cern.ch/Publications/Notes/netnote.ps.gz>
27. A. Fassò, A. Ferrari, J. Ranft, P.R. Sala, SARE-3 Workshop, KEK, Tsukuba, KEK Report Proceedings 97-5 (1997), p. 32, <http://fluka.web.cern.ch/fluka/>
28. CHARM collaboration, J.V. Allaby et al., Z. Phys. C **36**, 611 (1987)
29. CDHS collaboration, A. Blondel et al., Z. Phys. C **45**, 361 (1990)
30. CCFR Collaboration, K.S. McFarland et al., Eur. Phys. J. C **1**, 509 (1998)
31. CHORUS Collaboration, E. Eskut et al., Phys. Lett. B **503**, 1 (2001)
32. V. Barger, W.Y. Keung, R.J.N. Phillips, Phys. Lett. B **92**, 179 (1980)
33. J.P. Leveille, T. Weiler, Nucl. Phys. B **147**, 147 (1979)
34. G.J. Feldman, R.D. Cousins, Phys. Rev. D **57**, 3873 (1998)